

Beam-energy dependence of charge separation along the magnetic field in Au+Au collisions at RHIC

- L. Adamczyk,¹ J. K. Adkins,²³ G. Agakishiev,²¹ M. M. Aggarwal,³⁵ Z. Ahammed,⁵³ I. Alekseev,¹⁹ J. Alford,²² C. D. Anson,³² A. Aparin,²¹ D. Arkhipkin,⁴ E. C. Aschenauer,⁴ G. S. Averichev,²¹ A. Banerjee,⁵³ D. R. Beavis,⁴ R. Bellwied,⁴⁹ A. Bhasin,²⁰ A. K. Bhati,³⁵ P. Bhattarai,⁴⁸ H. Bichsel,⁵⁵ J. Bielcik,¹³ J. Bielcikova,¹⁴ L. C. Bland,⁴ I. G. Bordyuzhin,¹⁹ W. Borowski,⁴⁵ J. Bouchet,²² A. V. Brandin,³⁰ S. G. Brovko,⁶ S. Bültmann,³³ I. Bunzarov,²¹ T. P. Burton,⁴ J. Butterworth,⁴¹ H. Caines,⁵⁷ M. Calderón de la Barca Sánchez,⁶ D. Cebra,⁶ R. Cendejas,³⁶ M. C. Cervantes,⁴⁷ P. Chaloupka,¹³ Z. Chang,⁴⁷ S. Chattopadhyay,⁵³ H. F. Chen,⁴² J. H. Chen,⁴⁴ L. Chen,⁹ J. Cheng,⁵⁰ M. Cherney,¹² A. Chikanian,⁵⁷ W. Christie,⁴ J. Chwastowski,¹¹ M. J. M. Codrington,⁴⁸ G. Contin,²⁶ J. G. Cramer,⁵⁵ H. J. Crawford,⁵ X. Cui,⁴² S. Das,¹⁶ A. Davila Leyva,⁴⁸ L. C. De Silva,¹² R. R. Debbé,⁴ T. G. Dedovich,²¹ J. Deng,⁴³ A. A. Derevschikov,³⁷ R. Derradi de Souza,⁸ S. Dhamija,¹⁸ B. di Ruzza,⁴ L. Didenko,⁴ C. Dilks,³⁶ F. Ding,⁶ P. Djawotho,⁴⁷ X. Dong,²⁶ J. L. Drachenberg,⁵² J. E. Draper,⁶ C. M. Du,²⁵ L. E. Dunkelberger,⁷ J. C. Dunlop,⁴ L. G. Efimov,²¹ J. Engelage,⁵ K. S. Engle,⁵¹ G. Eppley,⁴¹ L. Eun,²⁶ O. Evdokimov,¹⁰ O. Eyser,⁴ R. Fatemi,²³ S. Fazio,⁴ J. Fedorisin,²¹ P. Filip,²¹ E. Finch,⁵⁷ Y. Fisyak,⁴ C. E. Flores,⁶ C. A. Gagliardi,⁴⁷ D. R. Gangadharan,³² D. Garand,³⁸ F. Geurts,⁴¹ A. Gibson,⁵² M. Girard,⁵⁴ S. Gliske,² L. Greiner,²⁶ D. Grosnick,⁵² D. S. Gunarathne,⁴⁶ Y. Guo,⁴² A. Gupta,²⁰ S. Gupta,²⁰ W. Guryn,⁴ B. Haag,⁶ A. Hamed,⁴⁷ L.-X. Han,⁴⁴ R. Haque,³¹ J. W. Harris,⁵⁷ S. Heppelmann,³⁶ A. Hirsch,³⁸ G. W. Hoffmann,⁴⁸ D. J. Hofman,¹⁰ S. Horvat,⁵⁷ B. Huang,⁴ H. Z. Huang,⁷ X. Huang,⁵⁰ P. Huck,⁹ T. J. Humanic,³² G. Igo,⁷ W. W. Jacobs,¹⁸ H. Jang,²⁴ E. G. Judd,⁵ S. Kabana,⁴⁵ D. Kalinkin,¹⁹ K. Kang,⁵⁰ K. Kauder,¹⁰ H. W. Ke,⁴ D. Keane,²² A. Kechechyan,²¹ A. Kesich,⁶ Z. H. Khan,¹⁰ D. P. Kikola,⁵⁴ I. Kisel,¹⁵ A. Kisiel,⁵⁴ D. D. Koetke,⁵² T. Kollegger,¹⁵ J. Konzer,³⁸ I. Koralt,³³ L. Kotchenda,³⁰ A. F. Kraishan,⁴⁶ P. Kravtsov,³⁰ K. Krueger,² I. Kulakov,¹⁵ L. Kumar,³¹ R. A. Kycia,¹¹ M. A. C. Lamont,⁴ J. M. Landgraf,⁴ K. D. Landry,⁷ J. Lauret,⁴ A. Lebedev,⁴ R. Lednický,²¹ J. H. Lee,⁴ M. J. LeVine,⁴ C. Li,⁴² W. Li,⁴⁴ X. Li,³⁸ X. Li,⁴⁶ Y. Li,⁵⁰ Z. M. Li,⁹ M. A. Lisa,³² F. Liu,⁹ T. Ljubicic,⁴ W. J. Llope,⁴¹ M. Lomnitz,²² R. S. Longacre,⁴ X. Luo,⁹ G. L. Ma,⁴⁴ Y. G. Ma,⁴⁴ D. M. M. D. Madagadgettige Don,¹² D. P. Mahapatra,¹⁶ R. Majka,⁵⁷ S. Margetis,²² C. Markert,⁴⁸ H. Masui,²⁶ H. S. Matis,²⁶ D. McDonald,⁴⁹ T. S. McShane,¹² N. G. Minaev,³⁷ S. Mioduszewski,⁴⁷ B. Mohanty,³¹ M. M. Mondal,⁴⁷ D. A. Morozov,³⁷ M. K. Mustafa,²⁶ B. K. Nandi,¹⁷ Md. Nasim,³¹ T. K. Nayak,⁵³ J. M. Nelson,³ G. Nigmatkulov,³⁰ L. V. Nogach,³⁷ S. Y. Noh,²⁴ J. Novak,²⁹ S. B. Nurushev,³⁷ G. Odyniec,²⁶ A. Ogawa,⁴ K. Oh,³⁹ A. Ohlson,⁵⁷ V. Okorokov,³⁰ E. W. Oldag,⁴⁸ D. L. Olvitt Jr.,⁴⁶ M. Pachr,¹³ B. S. Page,¹⁸ S. K. Pal,⁵³ Y. X. Pan,⁷ Y. Pandit,¹⁰ Y. Panebratsev,²¹ T. Pawlak,⁵⁴ B. Pawlik,³⁴ H. Pei,⁹ C. Perkins,⁵ W. Peryt,⁵⁴ P. Pile,⁴ M. Planinic,⁵⁸ J. Pluta,⁵⁴ N. Poljak,⁵⁸ J. Porter,²⁶ A. M. Poskanzer,²⁶ N. K. Pruthi,³⁵ M. Przybycien,¹ P. R. Pujahari,¹⁷ J. Putschke,⁵⁶ H. Qiu,²⁶ A. Quintero,²² S. Ramachandran,²³ R. Raniwala,⁴⁰ S. Raniwala,⁴⁰ R. L. Ray,⁴⁸ C. K. Riley,⁵⁷ H. G. Ritter,²⁶ J. B. Roberts,⁴¹ O. V. Rogachevskiy,²¹ J. L. Romero,⁶ J. F. Ross,¹² A. Roy,⁵³ L. Ruan,⁴ J. Rusnak,¹⁴ O. Rusnakova,¹³ N. R. Sahoo,⁴⁷ P. K. Sahu,¹⁶ I. Sakrejda,²⁶ S. Salur,²⁶ J. Sandweiss,⁵⁷ E. Sangaline,⁶ A. Sarkar,¹⁷ J. Schambach,⁴⁸ R. P. Scharenberg,³⁸ A. M. Schmah,²⁶ W. B. Schmidke,⁴ N. Schmitz,²⁸ J. Seger,¹² P. Seyboth,²⁸ N. Shah,⁷ E. Shahaliev,²¹ P. V. Shanmuganathan,²² M. Shao,⁴² B. Sharma,³⁵ W. Q. Shen,⁴⁴ S. S. Shi,²⁶ Q. Y. Shou,⁴⁴ E. P. Sichtermann,²⁶ R. N. Singaraju,⁵³ M. J. Skoby,¹⁸ D. Smirnov,⁴ N. Smirnov,⁵⁷ D. Solanki,⁴⁰ P. Sorensen,⁴ H. M. Spinka,² B. Srivastava,³⁸ T. D. S. Stanislaus,⁵² J. R. Stevens,²⁷ R. Stock,¹⁵ M. Strikhanov,³⁰ B. Stringfellow,³⁸ M. Sumner,¹⁴ X. Sun,²⁶ X. M. Sun,²⁶ Y. Sun,⁴² Z. Sun,²⁵ B. Surrow,⁴⁶ D. N. Svirida,¹⁹ T. J. M. Symons,²⁶ M. A. Szelezniak,²⁶ J. Takahashi,⁸ A. H. Tang,⁴ Z. Tang,⁴² T. Tarnowsky,²⁹ J. H. Thomas,²⁶ A. R. Timmins,⁴⁹ D. Tlusty,¹⁴ M. Tokarev,²¹ S. Trentalange,⁷ R. E. Tribble,⁴⁷ P. Tribedy,⁵³ B. A. Trzeciak,¹³ O. D. Tsai,⁷ J. Turnau,³⁴ T. Ullrich,⁴ D. G. Underwood,² G. Van Buren,⁴ G. van Nieuwenhuizen,²⁷ M. Vandenbroucke,⁴⁶ J. A. Vanfossen, Jr.,²² R. Varma,¹⁷ G. M. S. Vasconcelos,⁸ A. N. Vasiliev,³⁷ R. Vertesi,¹⁴ F. Videbæk,⁴ Y. P. Viyogi,⁵³ S. Vokal,²¹ S. A. Voloshin,⁵⁶ A. Vossen,¹⁸ M. Wada,⁴⁸ F. Wang,³⁸ G. Wang,⁷ H. Wang,⁴ J. S. Wang,²⁵ X. L. Wang,⁴² Y. Wang,⁵⁰ Y. Wang,¹⁰ G. Webb,²³ J. C. Webb,⁴ G. D. Westfall,²⁹ H. Wieman,²⁶ S. W. Wissink,¹⁸ R. Witt,⁵¹ Y. F. Wu,⁹ Z. Xiao,⁵⁰ W. Xie,³⁸ K. Xin,⁴¹ H. Xu,²⁵ J. Xu,⁹ N. Xu,²⁶ Q. H. Xu,⁴³ Y. Xu,⁴² Z. Xu,⁴ W. Yan,⁵⁰ C. Yang,⁴² Y. Yang,²⁵ Y. Yang,⁹ Z. Ye,¹⁰ P. Yepes,⁴¹ L. Yi,³⁸ K. Yip,⁴ I.-K. Yoo,³⁹ N. Yu,⁹ Y. Zawisza,⁴² H. Zbroszczyk,⁵⁴ W. Zha,⁴² J. B. Zhang,⁹ J. L. Zhang,⁴³ S. Zhang,⁴⁴ X. P. Zhang,⁵⁰ Y. Zhang,⁴²

Z. P. Zhang,⁴² F. Zhao,⁷ J. Zhao,⁹ C. Zhong,⁴⁴ X. Zhu,⁵⁰ Y. H. Zhu,⁴⁴ Y. Zoukarneeva,²¹ and M. Zyzak¹⁵
(STAR Collaboration)

- ¹AGH University of Science and Technology, Cracow, Poland
- ²Argonne National Laboratory, Argonne, Illinois 60439, USA
- ³University of Birmingham, Birmingham, United Kingdom
- ⁴Brookhaven National Laboratory, Upton, New York 11973, USA
- ⁵University of California, Berkeley, California 94720, USA
- ⁶University of California, Davis, California 95616, USA
- ⁷University of California, Los Angeles, California 90095, USA
- ⁸Universidade Estadual de Campinas, Sao Paulo, Brazil
- ⁹Central China Normal University (HZNU), Wuhan 430079, China
- ¹⁰University of Illinois at Chicago, Chicago, Illinois 60607, USA
- ¹¹Cracow University of Technology, Cracow, Poland
- ¹²Creighton University, Omaha, Nebraska 68178, USA
- ¹³Czech Technical University in Prague, FNSPE, Prague, 115 19, Czech Republic
- ¹⁴Nuclear Physics Institute AS CR, 250 68 Řež/Prague, Czech Republic
- ¹⁵Frankfurt Institute for Advanced Studies FIAS, Germany
- ¹⁶Institute of Physics, Bhubaneswar 751005, India
- ¹⁷Indian Institute of Technology, Mumbai, India
- ¹⁸Indiana University, Bloomington, Indiana 47408, USA
- ¹⁹Alikhanov Institute for Theoretical and Experimental Physics, Moscow, Russia
- ²⁰University of Jammu, Jammu 180001, India
- ²¹Joint Institute for Nuclear Research, Dubna, 141 980, Russia
- ²²Kent State University, Kent, Ohio 44242, USA
- ²³University of Kentucky, Lexington, Kentucky, 40506-0055, USA
- ²⁴Korea Institute of Science and Technology Information, Daejeon, Korea
- ²⁵Institute of Modern Physics, Lanzhou, China
- ²⁶Lawrence Berkeley National Laboratory, Berkeley, California 94720, USA
- ²⁷Massachusetts Institute of Technology, Cambridge, Massachusetts 02139-4307, USA
- ²⁸Max-Planck-Institut für Physik, Munich, Germany
- ²⁹Michigan State University, East Lansing, Michigan 48824, USA
- ³⁰Moscow Engineering Physics Institute, Moscow Russia
- ³¹National Institute of Science Education and Research, Bhubaneswar 751005, India
- ³²Ohio State University, Columbus, Ohio 43210, USA
- ³³Old Dominion University, Norfolk, Virginia 23529, USA
- ³⁴Institute of Nuclear Physics PAN, Cracow, Poland
- ³⁵Panjab University, Chandigarh 160014, India
- ³⁶Pennsylvania State University, University Park, Pennsylvania 16802, USA
- ³⁷Institute of High Energy Physics, Protvino, Russia
- ³⁸Purdue University, West Lafayette, Indiana 47907, USA
- ³⁹Pusan National University, Pusan, Republic of Korea
- ⁴⁰University of Rajasthan, Jaipur 302004, India
- ⁴¹Rice University, Houston, Texas 77251, USA
- ⁴²University of Science and Technology of China, Hefei 230026, China
- ⁴³Shandong University, Jinan, Shandong 250100, China
- ⁴⁴Shanghai Institute of Applied Physics, Shanghai 201800, China
- ⁴⁵SUBATECH, Nantes, France
- ⁴⁶Temple University, Philadelphia, Pennsylvania 19122, USA
- ⁴⁷Texas A&M University, College Station, Texas 77843, USA
- ⁴⁸University of Texas, Austin, Texas 78712, USA
- ⁴⁹University of Houston, Houston, Texas 77204, USA
- ⁵⁰Tsinghua University, Beijing 100084, China
- ⁵¹United States Naval Academy, Annapolis, Maryland, 21402, USA
- ⁵²Valparaiso University, Valparaiso, Indiana 46383, USA
- ⁵³Variable Energy Cyclotron Centre, Kolkata 700064, India
- ⁵⁴Warsaw University of Technology, Warsaw, Poland
- ⁵⁵University of Washington, Seattle, Washington 98195, USA
- ⁵⁶Wayne State University, Detroit, Michigan 48201, USA
- ⁵⁷Yale University, New Haven, Connecticut 06520, USA
- ⁵⁸University of Zagreb, Zagreb, HR-10002, Croatia

Local parity-odd domains are theorized to form inside a Quark-Gluon-Plasma (QGP) which has been produced in high-energy heavy-ion collisions. The local parity-odd domains manifest themselves as charge separation along the magnetic field axis via the chiral magnetic effect (CME). The experimental observation of charge separation has previously been reported for heavy-ion collisions at the top RHIC energies. In this paper, we present the results of the beam-energy dependence of the charge correlations in Au+Au collisions at midrapidity for center-of-mass energies of 7.7, 11.5, 19.6, 27, 39 and 62.4 GeV from the STAR experiment. After background subtraction, the signal gradually reduces with decreased beam energy, and tends to vanish by 7.7 GeV. The implications of these results for the CME will be discussed.

PACS numbers: 25.75.-q

The strong interaction is parity even at vanishing temperature and isospin density [1], but parity could be violated locally in microscopic domains in QCD at finite temperature as a consequence of topologically non-trivial configurations of gauge fields [2, 3]. The Relativistic Heavy Ion Collider (RHIC) provides a good opportunity to study such parity-odd (\mathcal{P} -odd) domains, where the local imbalance of chirality results from the interplay of these topological configurations with the hot, dense and deconfined Quark-Gluon-Plasma (QGP) created in heavy-ion collisions.

The \mathcal{P} -odd domains can be manifested via the chiral magnetic effect (CME). In heavy-ion collisions, energetic protons (mostly spectators) produce a magnetic field (B) with a strength that peaks around $eB \approx 10^4 \text{ MeV}^2$ [4]. The collision geometry is illustrated in Fig. 1. The strong magnetic field, coupled with the chiral asymmetry in the \mathcal{P} -odd domains, induces a separation of electric charge along the direction of the magnetic field [4–9]. Based on data from the STAR [10–13] and PHENIX [14, 15] collaborations at RHIC and the ALICE collaboration [16] at the LHC, charge-separation fluctuations have been experimentally observed. The interpretation of these data as an indication of the CME is still under intense discussion, see e.g. [13, 17, 18] and references therein. A study of the beam-energy dependence of the charge separation effect will shed light on the interpretation of the data.

The magnetic field axis points in the direction that is perpendicular to the reaction plane, which contains the impact parameter and the beam momenta. Experimentally the charge separation is measured perpendicular to the reaction plane with a three-point correlator, $\gamma \equiv \langle \cos(\phi_1 + \phi_2 - 2\Psi_{\text{RP}}) \rangle$ [19]. In Fig. 1, ϕ and Ψ_{RP} denote the azimuthal angles of a particle and the reaction plane, respectively. In practice, we approximate the reaction plane with the “event plane” (Ψ_{EP}) reconstructed with measured particles, and then correct the measurement for the finite event plane resolution [10–12].

This Letter reports measurements of the three-point correlator, γ , for charged particles produced in Au+Au collisions. 8M events were analyzed at the center-of-mass energy $\sqrt{s_{\text{NN}}} = 62.4 \text{ GeV}$ (2005), 100M at 39 GeV (2010), 46M at 27 GeV (2011), 20M at 19.6 GeV (2011), 10M at 11.5 GeV (2010) and 4M at 7.7 GeV (2010). Events selected with a minimum bias trigger have

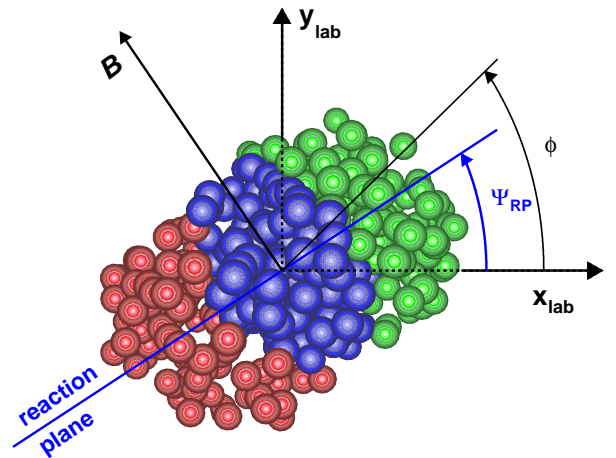


FIG. 1: (Color online) Schematic depiction of the transverse plane for a collision of two heavy ions (the left one emerging from and the right one going into the page). Particles are produced in the overlap region (blue-colored nucleons). The azimuthal angles of the reaction plane and a produced particle used in the three-point correlator, γ , are depicted here.

been sorted into centrality classes based on uncorrected charged particle multiplicity at midrapidity. Charged particle tracks in this analysis were reconstructed in the STAR Time Projection Chamber (TPC) [20], within a pseudorapidity range of $|\eta| < 1$ and a transverse momentum range of $0.15 < p_T < 2 \text{ GeV}/c$. The centrality definition and track quality cuts are the same as in Refs. [21], unless otherwise specified. Only events within 40 cm of the center of the detector along the beam direction were selected for data sets at $\sqrt{s_{\text{NN}}} = 19.6 - 62.4 \text{ GeV}$. This cut was 50 and 70 cm for 11.5 and 7.7 GeV collisions, respectively. To suppress events from collisions with the beam pipe (radius 3.95 cm), only those events with a radial position of the reconstructed primary vertex within 2 cm were analyzed. A cut on the distance of closest approach to the primary vertex (DCA) $< 2 \text{ cm}$ was also applied to reduce the number of weak decay tracks or secondary interactions. The experimental observables involved in the analysis have been corrected for the particle track reconstruction efficiency.

In an event, charge separation along the magnetic field

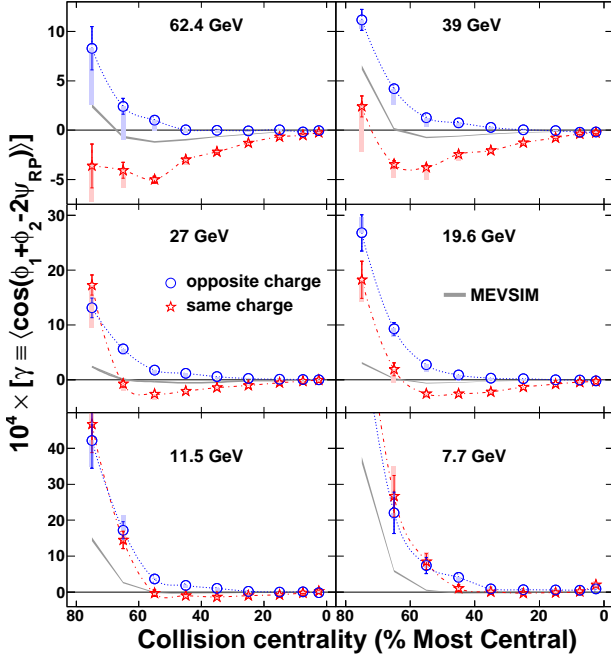


FIG. 2: (Color online) The three-point correlator, γ , as a function of centrality for Au+Au collisions at 7.7 – 62.4 GeV. Note that the vertical scales are different for different rows. The filled boxes (starting from the central values) represent one type of systematic uncertainty (as discussed in the text). Charge independent results from the model calculations of MEVSIM [27] are also shown with grey curves.

(i.e., perpendicular to the reaction plane) may be described phenomenologically by a sine term in the Fourier decomposition of the charged particle azimuthal distribution,

$$\frac{dN_\alpha}{d\phi} \propto 1 + 2v_1 \cos(\Delta\phi) + 2a_\alpha \sin(\Delta\phi) + 2v_2 \cos(2\Delta\phi) + \dots \quad (1)$$

where $\Delta\phi = \phi - \Psi_{RP}$, and the subscript α (+ or -) denotes the charge sign of particles. Conventionally v_1 is called “directed flow” and v_2 “elliptic flow”, and they describe the collective motion of the produced particles [22]. The parameter a (with $a_- = -a_+$) quantifies the \mathcal{P} -violating effect. If spontaneous parity violation occurs, then the signs of a_+ and a_- will vary from event to event, leading to $\langle a_+ \rangle = \langle a_- \rangle = 0$. In the expansion of the three-point correlator, $\gamma = \langle \cos(\Delta\phi_1) \cos(\Delta\phi_2) - \sin(\Delta\phi_1) \sin(\Delta\phi_2) \rangle$, the second term contains the fluctuation term $-\langle a_\pm a_\pm \rangle$, which may be non-zero when accumulated over particle pairs of separate charge combinations. The first term ($\langle \cos(\Delta\phi_1) \cos(\Delta\phi_2) \rangle$) in the expansion provides a baseline unrelated to the magnetic field.

The reaction plane of a heavy-ion collision is not known a priori, and in practice it is approximated with an event plane which is reconstructed from particle azimuthal dis-

tributions [22]. In this analysis, we exploited the large elliptic flow of charged hadrons produced at mid-rapidity to construct the event plane angle:

$$\Psi_{EP} = \frac{1}{2} \tan^{-1} \left[\frac{\sum \omega_i \sin(2\phi_i)}{\sum \omega_i \cos(2\phi_i)} \right], \quad (2)$$

where ω_i is a weight for each particle i in the sum [22]. The weight was chosen to be the p_T of the particle itself, and only particles with $p_T < 2$ GeV/c were used. Although the STAR TPC has good azimuthal symmetry, small acceptance effects in the calculation of the event plane azimuth were removed by the method of shifting [23]. The observed correlations were corrected for the event plane resolution, estimated with the correlation between two random sub-events (details in Ref. [22]).

The event plane thus obtained from the produced particles is sometimes called “the participant plane” since it is subject to the event-by-event fluctuations of the initial participant nucleons [24]. A better approximation to the reaction plane could be obtained from the spectator neutron distributions detected in the STAR zero degree calorimeters (ZDC-SMDs) [25]. This type of event plane utilizes the directed flow of spectator neutrons measured at very forward rapidity. We have measured the three point correlations using both types of reaction plane estimates and the results are consistent with each other [12]. Other systematic uncertainties were studied extensively and discussed in our previous publications on the subject [10, 11]. All were shown to be negligible compared with the uncertainty in determining the reaction plane. In this work, we have only used the participant plane because the efficiency of ZDC-SMDs becomes low for low beam energies.

Figure 2 presents the opposite-charge (γ_{OS}) and same-charge (γ_{SS}) correlators for Au+Au collisions at $\sqrt{s_{NN}} = 7.7 - 62.4$ GeV as a function of centrality (0 means the most central collisions). In most cases, the ordering of γ_{OS} and γ_{SS} is the same as in Au+Au (Pb+Pb) collisions at higher energies [10–12, 16], suggesting charge-separation fluctuations perpendicular to the reaction plane. As a systematic check, the charge combinations of ++ and -- were always found to be consistent with each other (not shown here). With decreased beam energy, both γ_{OS} and γ_{SS} tend to rise up in peripheral collisions. This feature seems to be charge independent, and can be explained by momentum conservation and elliptic flow [12]. Momentum conservation forces all produced particles, regardless of charge, to separate from each other, while elliptic flow, a collective motion, works in the opposite sense. For peripheral collisions, the multiplicity (N) is small, and momentum conservation dominates. At lower beam energies, N also becomes smaller and hence higher values for γ_{OS} and γ_{SS} . For more central collisions where the multiplicity is large, this type of \mathcal{P} -even background can be estimated as $-v_2/N$ [12, 26]. In Fig. 2, we also show the model calculations of MEVSIM,

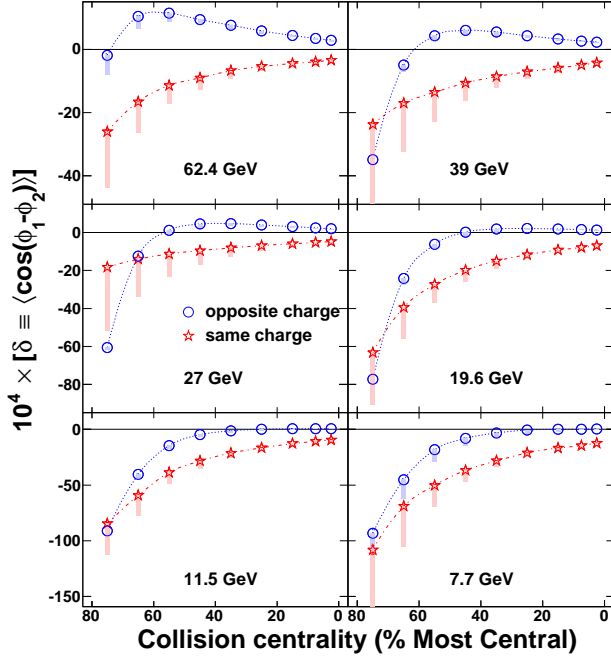


FIG. 3: (Color online) The two-particle correlation as a function of centrality for Au+Au collisions at 7.7–62.4 GeV. Note that the vertical scales are different for different rows. The filled boxes bear the same meaning as those in Fig 2 and are described in the text.

a Monte Carlo event generator with an implementation of v_2 and momentum conservation, developed for STAR simulations [27]. The model results qualitatively describe the beam-energy dependency of the charge-independent background.

In view of the charge-independent background, the charge separation effect can be studied via the difference between γ_{OS} and γ_{SS} . The difference ($\gamma_{OS} - \gamma_{SS}$) remains positive for all centralities down to the beam energy ~ 19.6 GeV, and the magnitude decreases from peripheral to central collisions. Presumably this is partially owing to the reduced magnetic field and partially owing to the more pronounced dilution effect in more central collisions. A dilution of the correlation is expected when there are multiple sources involved in the collision [11, 28]. The difference between γ_{OS} and γ_{SS} approaches zero in peripheral collisions at lower energies, especially at 7.7 GeV, which could be understood in terms of the CME hypothesis if the formation of the QGP becomes less likely in peripheral collisions at low beam energies [29].

The systematic uncertainties of ($\gamma_{OS} - \gamma_{SS}$) due to the analysis cuts, the track reconstruction efficiency and the event plane determination were estimated to be approximately 10%, 5% and 10%, respectively. Overall, total systematic uncertainties are typically 15%, except for the cases where ($\gamma_{OS} - \gamma_{SS}$) is close to zero. Another type of uncertainty is due to quantum interference

(“HBT” effects) and final-state-interactions (Coulomb dominated) [12], which are most prominent for low relative momenta. To suppress the contributions from these effects, we applied the conditions of $\Delta p_T > 0.15$ GeV/c and $\Delta\eta > 0.15$ to the correlations, shown with filled boxes in Figs. 2, 3 and 4. The boxes start from the central values with default conditions and end with the results with the above extra conditions on Δp_T and $\Delta\eta$.

Interpretation of the three particle correlation result, γ , requires additional information such as a measurement of the two particle correlation $\delta \equiv \langle \cos(\phi_1 - \phi_2) \rangle = \langle \cos(\Delta\phi_1) \cos(\Delta\phi_2) + \sin(\Delta\phi_1) \sin(\Delta\phi_2) \rangle$. The expansion of δ also contains the fluctuation term $\langle a_{\pm} a_{\pm} \rangle$. Figure 3 shows δ as a function of centrality for Au+Au collisions at 7.7–62.4 GeV. In most cases, δ_{OS} is above δ_{SS} , indicating an overwhelming background, larger than any possible CME effect. The background sources, if coupled with collective flow, will also contribute to γ . Taking this into account, we can express γ and δ in the following forms, where the unknown parameter κ , as argued in Ref. [30], is of the order of unity.

$$\gamma \equiv \langle \cos(\phi_1 + \phi_2 - 2\Psi_{RP}) \rangle = \kappa v_2 F - H \quad (3)$$

$$\delta \equiv \langle \cos(\phi_1 - \phi_2) \rangle = F + H, \quad (4)$$

where H and F are the CME and background contributions, respectively. In Ref. [30] $\kappa = 1$, but it could deviate from unity owing to a finite detector acceptance and other theoretical uncertainties. We can solve for H from Eqns. 3 and 4,

$$H^{\kappa} = (\kappa v_2 \delta - \gamma) / (1 + \kappa v_2). \quad (5)$$

Figure 4 shows $H_{SS} - H_{OS}$ as a function of beam energy for three centrality bins in Au+Au collisions. v_2 for the beam energies under study has been measured in our previous publications [21]. The default values (dotted curves) are for $H^{\kappa=1}$, and the solid (dash-dot) curves are obtained with $\kappa = 1.5$ ($\kappa = 2$). For comparison, the results for 10–60% Pb+Pb collisions at 2.76 TeV are also shown [16]. The ($H_{SS} - H_{OS}$) curve for $\kappa = 1$ suggests a non-zero charge separation effect with a weak energy dependence above 19.6 GeV, but the trend rapidly decreases to zero in the interval between 19.6 and 7.7 GeV. This may be explained by the probable domination of hadronic interactions over partonic ones at low beam energies. With increased κ , ($H_{SS} - H_{OS}$) decreases for all beam energies and may even totally disappear in some case (e.g. with $\kappa \sim 2$ in 10–30% collisions). A better theoretical estimate of κ in the future would enable us to extract a firmer conclusion from the data presented.

In summary, an analysis of the three-point correlation between two charged particles and the reaction plane has been carried out for Au+Au collisions at $\sqrt{s_{NN}} = 7.7$ –62.4 GeV. The general trend of the correlations (γ_{OS} and γ_{SS}), as a function of centrality and beam energy, can be qualitatively described by the model calculations

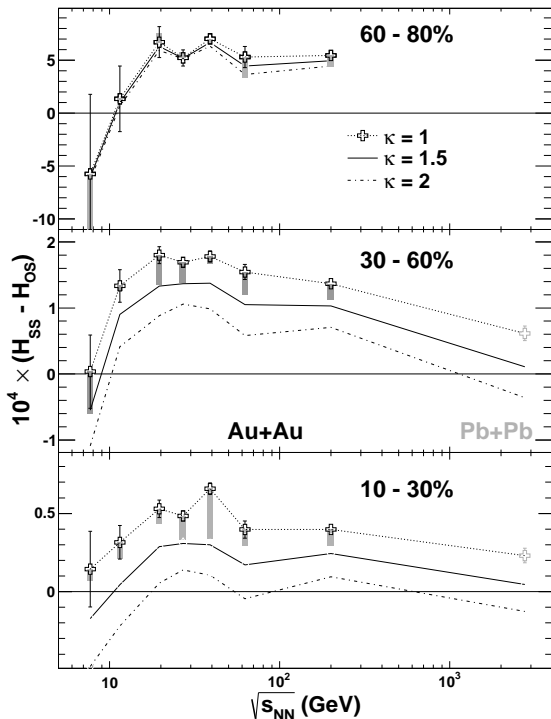


FIG. 4: $H_{SS} - H_{OS}$, as a function of beam energy for three centrality bins in Au+Au collisions. The default values (dotted curves) are for $H^{\kappa=1}$, and the solid (dash-dot) curves are obtained with $\kappa = 1.5$ ($\kappa = 2$). For comparison, the results for Au+Au collisions at 200 GeV [11] and Pb+Pb collisions at 2.76 TeV [16] are also shown. The systematic errors of the STAR data (filled boxes) bear the same meaning as those in Fig. 2.

of MEVSIM. This result indicates a large contribution from the \mathcal{P} -even background due to momentum conservation and collective flow. The charge separation along the magnetic field, studied via $(H_{SS} - H_{OS})$, shows a signal with a weak energy dependence down to 19.6 GeV and then falls steeply at lower energies. This trend may be consistent with the hypothesis of local parity violation because there should be a smaller probability for the CME at lower energies where the hadronic phase plays a more dominant role than the partonic phase. A more definitive result may be obtained in the future if we can increase the statistics by a factor of ten for the low energies and if we can reduce the uncertainty associated with determination of the value of κ .

We thank the RHIC Operations Group and RCF at BNL, the NERSC Center at LBNL, the KISTI Center in Korea and the Open Science Grid consortium for providing resources and support. This work was supported in part by the Offices of NP and HEP within the U.S. DOE Office of Science, the U.S. NSF, CNRS/IN2P3, FAPESP CNPq of Brazil, Ministry of Ed. and Sci. of the Russian Federation, NNSFC, CAS, MoST and MoE of China, the Korean Research Foundation, GA and MSMT

of the Czech Republic, FIAS of Germany, DAE, DST, and CSIR of India, National Science Centre of Poland, National Research Foundation (NRF-2012004024), Ministry of Sci., Ed. and Sports of the Rep. of Croatia, and RosAtom of Russia.

-
- [1] C. Vafa and E. Whitten, Phys. Rev. Lett. **53**, 535 (1984).
 - [2] T. D. Lee, Phys. Rev. D **8**, 1226 (1973).
 - [3] T. D. Lee and G. C. Wick, Phys. Rev. D **9**, 2291 (1974).
 - [4] D. E. Kharzeev, L. D. McLerran and H. J. Warringa, Nucl. Phys. A **803**, 227 (2008).
 - [5] D. Kharzeev, Phys. Lett. B **633**, 260 (2006).
 - [6] D. Kharzeev and A. Zhitnitsky, Nucl. Phys. A **797**, 67 (2007).
 - [7] K. Fukushima, D. E. Kharzeev and H. J. Warringa, Phys. Rev. D **78**, 074033 (2008).
 - [8] D. E. Kharzeev, Annals Phys. **325**, 205 (2010).
 - [9] R. Gatto and M. Ruggieri, Phys. Rev. D **85**, 054013 (2012).
 - [10] B. I. Abelev *et al.* [STAR Collaboration], Phys. Rev. Lett. **103**, 251601 (2009).
 - [11] B. I. Abelev *et al.* [STAR Collaboration], Phys. Rev. C **81**, 054908 (2010).
 - [12] L. Adamczyk *et al.* [STAR Collaboration], Phys. Rev. C **88**, 064911 (2013).
 - [13] L. Adamczyk *et al.* [STAR Collaboration], arXiv:1303.0901, accepted by Phys. Rev. C.
 - [14] N. N. Ajitanand, S. Esumi, R. A. Lacey [PHENIX Collaboration], in: Proc. of the RBRC Workshops, vol. 96, 2010: "P- and CP-odd effects in hot and dense matter".
 - [15] N. N. Ajitanand, R. A. Lacey, A. Taranenko and J. M. Alexander, Phys. Rev. C **83**, 011901 (2011).
 - [16] B. I. Abelev *et al.* [ALICE Collaboration], Phys. Rev. Lett. **110**, 012301 (2013).
 - [17] A. Bzdak, V. Koch and J. Liao, Phys. Rev. C **81**, 031901 (2010); Phys. Rev. C **82**, 054902 (2010).
 - [18] D. E. Kharzeev and D. T. Son, Phys. Rev. Lett. **106**, 062301 (2011).
 - [19] S. Voloshin, Phys. Rev. C **70**, 057901 (2004).
 - [20] M. Anderson *et al.*, Nucl. Instr. Meth. A **499**, 659 (2003).
 - [21] J. Adams *et al.* [STAR Collaboration], Phys. Rev. C **72**, 014904 (2005); G. Agakishiev *et al.* [STAR Collaboration], Phys. Rev. C **86**, 014904 (2012); L. Adamczyk *et al.* [STAR Collaboration], Phys. Rev. C **86**, 054908 (2012).
 - [22] A. M. Poskanzer and S. A. Voloshin, Phys. Rev. C **58**, 1671 (1998).
 - [23] J. Barrette *et al.*, Phys. Rev. C **56**, 3254 (1997).
 - [24] J. -Y. Ollitrault, A. M. Poskanzer and S. A. Voloshin, Phys. Rev. C **80**, 014904 (2009).
 - [25] B. I. Abelev *et al.* [STAR Collaboration], Phys. Rev. Lett. **101**, 252301 (2008); and references therein.
 - [26] A. Bzdak, V. Koch and J. Liao, Phys. Rev. C **83**, 014905 (2011).
 - [27] R. L. Ray and R. S. Longacre, arXiv:nucl-ex/0008009 and private communication.
 - [28] G. -L. Ma and B. Zhang, Phys. Lett. **B700**, 39 (2011).
 - [29] V. A. Okorokov, Int. J. Mod. Phys. E **22**, 1350041 (2013).
 - [30] A. Bzdak, V. Koch and J. Liao, Lect. Notes Phys. **871**, 503 (2013).